

# Structural details of urea binding to barnase: a molecular dynamics analysis

Amedeo Caflisch<sup>1\*</sup> and Martin Karplus<sup>2,3\*</sup>

**Background:** The molecular mechanism of urea-induced protein unfolding has not been established. It is generally thought that denaturation results from the stabilizing interactions of urea with portions of the protein that are buried in the native state and become exposed upon unfolding of the protein.

**Results:** We have performed molecular dynamics simulations of barnase (a 110 amino acid RNase from *Bacillus amyloliquefaciens*) with explicit water and urea molecules at 300K and 360K. The native conformation was unaffected in the 300K simulations at neutral and low pH. Two of the three runs at 360K and low pH showed some denaturation, with partial unfolding of the hydrophobic core 2. The first solvation shell has a much higher density of urea molecules (water/urea ratio ranging from 2.07 to 2.73) than the bulk (water/urea ratio of 4.56). About one half of the first-shell urea molecules are involved in hydrogen bonds with polar or charged groups on the barnase surface, and between 15% and 18% of the first-shell urea molecules participate in multiple hydrogen bonds with barnase. The more stably bound urea molecules tend to be in crevices or pockets on the barnase surface.

**Conclusions:** The simulation results indicate that an aqueous urea solution solvates the surface of a polypeptide chain more favorably than pure water. Urea molecules interact more favorably with nonpolar groups of the protein than water does, and the presence of urea improves the interactions of water molecules with the hydrophilic groups of the protein. The results suggest that urea denaturation involves effects on both nonpolar and polar groups of proteins.

## Introduction

Urea,  $\text{CO}(\text{NH}_2)_2$ , is one of the most commonly used chemical denaturants of proteins. The aqueous solubility of protein mainchains and sidechains increases with increasing urea concentration [1,2]. An approximately linear relationship has been observed between the change in the unfolding free energy and the urea concentration with a proportionality constant that is related to the exposed surface area [3,4]. There are two main models for the origin of the urea stabilization. In one, the dominant effect of urea arises from the fact that it interacts more strongly with protein polar groups than water does. In fact, a study by Robinson and Jencks in 1965 [5] found that urea (8 M) causes a 3.2-fold increase in solubility of acetyltetraglycine ethyl ester (ATGEE) [5], a model system that is representative of the protein mainchain because it consists mainly of amide groups. They also found that the enthalpy and entropy of the urea–ATGEE interactions are negative, and they proposed that the direct interaction of urea with the ATGEE polar groups via multiple hydrogen bonds is responsible for the ‘nonhydrophobic’ effect of the chemical denaturants of the urea–guanidinium class [5]. Recent calorimetric studies have shown that the binding of urea

(and guanidinium chloride) to ribonuclease A, hen egg white lysozyme, and cytochrome *c* causes a significant decrease of the enthalpy and entropy of the system [6]. From the magnitude of the enthalpic term (–2.2 kcal/mol) and a correlation analysis of the number of urea-binding sites and structural characteristics of the three aforementioned proteins, the authors suggested that the binding sites for urea are formed by more than one hydrogen-bonding group [6], in accordance with the suggestion of Robinson and Jencks. In the second model, urea is presumed to stabilize hydrophobic groups in water by forming partial clathrates around them with less perturbation of the water structure than that involved in corresponding clathrates formed by water molecules [7,8]. From measurements of the free energy of transfer of amino acids with apolar sidechains from water to 8 M urea, Whitney and Tanford deduced that aqueous urea solutions can better accommodate hydrophobic amino acids than pure water can [7].

One approach to the problem of the interaction of urea with proteins is based on experimental studies of the structures of urea-containing systems. X-ray analysis of the

Addresses: <sup>1</sup>Department of Biochemistry, University of Zürich, Winterthurerstrasse 190, CH-8057 Zürich, Switzerland, <sup>2</sup>Laboratoire de Chimie Biophysique, Institut Le Bel, Université Louis Pasteur, F-6700 Strasbourg, France and <sup>3</sup>Department of Chemistry and Chemical Biology, Harvard University, 12 Oxford Street, Cambridge, MA 02140, USA.

\*Corresponding authors.  
E-mail: caflisch@bioc.unizh.ch  
marci@tammy.harvard.edu

**Key words:** barnase, folding, hydrophobic effect, solvation, urea

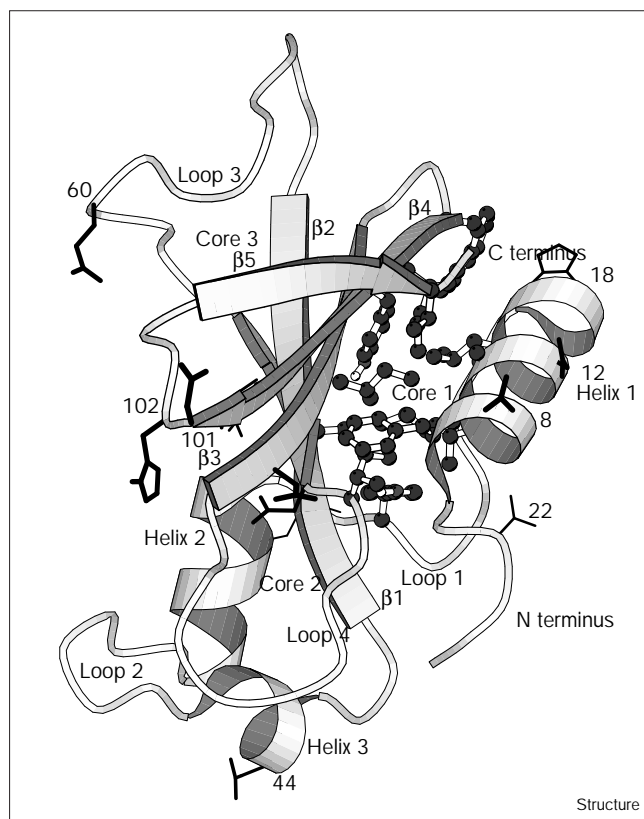
Received: 11 September 1998  
Revisions requested: 12 January 1999  
Revisions received: 1 February 1999  
Accepted: 10 February 1999

Published: 23 April 1999

Structure May 1999, 7:477–488  
<http://biomednet.com/elecref/0969212600700477>

© Elsevier Science Ltd ISSN 0969-2126

Figure 1



Ribbon representation of the backbone atoms of barnase emphasizing the secondary structural elements. Sidechains of hydrophobic core 1 are plotted in ball-and-stick representation. The sidechains that are affected by lowering the pH are shown in a stick representation with depth-dependent thickness; they are: Asp8, Asp12, His18, Asp22, Glu29, Asp44, Asp54, Glu60, Glu73, Asp75, Asp86, Asp101, and His102. The secondary structural elements include the following residues: N terminus (1–5), helix 1 (6–18), loop 1 (19–25), helix 2 (26–34), loop 2 (35–40), helix 3 (41–45), type II  $\beta$  turn (46–49), strand 1 (50–55), loop 3 (56–69), strand 2 (70–75), loop 4 (76–84), strand 3 (85–90), type I  $\beta$  turn (91–94), strand 4 (95–100), type III'  $\beta$  turn (101–104), strand 5 (105–108), C terminus (109–110). The Figure was made with the program MOLSCRIPT [39].

cocrystal structure of urea with 2,5-diketopiperazine (cyclic diglycine) revealed that five urea molecules surround a diketopiperazine molecule and form a total of eight hydrogen bonds with it [9]. Structural data on the interaction of urea with proteins are very limited. High resolution X-ray structures of hen egg white lysozyme crystals grown in the presence of 0, 0.7, 2, 3, 4, and 5 M urea and from crystals soaked in 9 M urea have shown that the urea molecules interact via multiple hydrogen bonds, mainly to the peptide groups but also with polar sidechains, while the conformation of the enzyme is practically unchanged [10]. Many of the urea molecules observed in the lysozyme crystals are involved in hydrogen bonds with two symmetry-related protein molecules. Recently, the binding of urea

to bovine pancreatic trypsin inhibitor (BPTI) and the acidic protein PEC-60 has been investigated by nuclear magnetic resonance (NMR) spectroscopy [11]. The conformations of these proteins were unaffected in the temperature range from 4 to 36°C and urea concentrations of up to 8 M at neutral pH. Preferential binding of urea to pockets and grooves on the protein surfaces was suggested on the basis of urea–protein intermolecular nuclear Overhauser effects (NOE) at 4°C. These NOE's disappeared at higher temperatures, indicating that exchange was occurring on a nanosecond time scale [11].

Given the limited experimental information available on the structural aspects of urea denaturation, it is useful to perform molecular dynamics simulations of urea/water solutions and of proteins in solution in the presence of urea molecules. Levitt and coworkers performed twelve 1 ns simulations of urea/water solutions with molarity values ranging from 0.23 to 6.71 M and compared them with shorter simulations of acetamide/water, acetone/water, isopropanol/water, and isobutylene/water solutions [12]. In the urea solutions there were more hydrogen bonds per water molecule than in the solutions with the less polar co-solvents because of a larger number of urea–water hydrogen bonds. They also found that urea mixes well with water and suggested that urea molecules decrease the free energy required to solvate hydrophobic groups [12]. In this paper we describe the results of molecular dynamics studies of barnase in an 8 M urea aqueous solution. Barnase is a particularly good system for study; it consists of three  $\alpha$  helices and a five-stranded  $\beta$  sheet, which are stabilized by three hydrophobic cores (Figure 1). Both its crystal structure [13,14] and its structure in solution are known [15]. Moreover, a wide range of detailed experimental [16,17] and theoretical [18] studies of barnase folding and unfolding have been made. Fersht and coworkers have used urea as well as guanidinium HCl in their work. We report here the results of several simulations at different temperatures (300 and 360 K) and pHs (neutral and acidic) and use them to analyze the interactions of urea with the folded protein and the protein at early stages of unfolding. The simulation results suggest that both models of the stabilizing interactions between urea and the polypeptide chain are valid. This is in agreement with solubility studies of amino acids [8].

While this work was in progress Tirado-Rives *et al.* [19] reported simulations of barnase in the presence of urea. Our results and conclusions complement their work. In the concluding discussion we present some comparisons and outline certain important differences in the results and in the interpretation.

## Results

### Global behavior

As found previously [18], barnase is stable over the time range of the control run (simulation W: CHARMM 22

all-hydrogen parameter set, 300K, neutral pH, pure water). During the last 200 ps the C $\alpha$  root mean square deviation (rmsd) from the X-ray structure never exceeds 1.36 Å and the average value is 1.12 Å; the heavy atom rmsd is 1.59 Å over the last 200 ps with a maximum of 1.78 Å. The radius of gyration ( $R_g$ ) averaged over the last 200 ps is 13.9 Å, which is close to the value of  $R_g$  for the X-ray structure (13.6 Å). The overall conformation, hydrophobic core compactness, and secondary structural elements are stable. We do not describe the structural details of the simulation results here because they are essentially the same as reported previously [18]. There are between two and three water molecules in core 2, in agreement with our previous simulations and with experimental results [13].

For the simulations in 8 M aqueous urea solution, the values of  $R_g$  and the C $\alpha$  rmsd from the X-ray structure as a function of time are shown in Figures 2a and 2b. The simulations U, UT360, and UlowpH are stable over the 700 ps time range, even though barnase experimentally undergoes reversible unfolding by heat ( $T_m = 324\text{K}$  at pH 4.4 [20]) or urea ([urea] $_m = 4.58\text{ M}$  [21]). The values of the C $\alpha$  and heavy-atom rmsds from the X-ray structure averaged over the last 200 ps are 1.10 and 1.56 Å, 1.59 and 2.08 Å, 1.58 and 2.18 Å, for the simulation U, UT360, and UlowpH, respectively. The N terminus and loops 2, 3, and 4 show the largest mainchain deviations from the X-ray structure (Figure 2c). A significant difference is also present in the N-terminal region of helix 2, whereas all of the other regular secondary structure elements are very stable. This is consistent with X-ray crystallographic data where it was found that the largest differences in the structures of lysozyme crystals grown in 0 and 5 M urea involved the surface loops, the active-site loop, and the C terminus [10]. The control run in the absence of urea (W) and the simulation U with urea show similar mainchain deviations from the X-ray structure, apart from the type II  $\beta$  turn between helix 3 and strand 1 (residues 46–49), which deviates in the simulation U but not in W (Figure 2d). The increases in the rmsds for the UT360 and UlowpH simulations are larger than for the control run W, but not large enough to indicate an onset of denaturation. This indicates that the barrier to unfolding in urea at 300 and 360K and in urea at low pH at 300K is such that the unfolding time is longer than the simulation time of 700 to 870 ps. This is much shorter than the experimental denaturation times under similar conditions; they are in the millisecond time range [22].

All three simulations with urea at 360K and low pH showed an increase in the C $\alpha$  rmsd;  $R_g$  increased in Uden2 and Uden3 but did not increase significantly in Uden1. The results for Uden1 are consistent with the fact that the largest deviations are localized in the loops and the N-terminal region of helix 2 (Figure 2c). A partial

expansion and increase in solvent accessibility of hydrophobic core 2 is the major conformational change in Uden2 and Uden3 (Figure 2e). This is in agreement with our previous simulations at high temperature (600K) and low pH (360K) performed with a different force field (polar-hydrogen approximation [23]) where it was found that core 2 is the least stable region of barnase [18,24]. The expansion of core 2 in Uden2 and Uden3 is due to the partial separation of the Tyr78, Trp35, and Leu33 sidechains. These sidechains were the first to separate from core 2 in our previous simulations [18]. In the last 50 ps of Uden2, core 2 contains on average ( $\pm$  standard deviation) 4.8 ( $\pm$  1.5) water molecules and 0.9 ( $\pm$  0.3) urea molecules, whereas during the final 50 ps of Uden3 there are 2.6 ( $\pm$  0.7) water molecules and 0.2 ( $\pm$  0.4) urea molecules in core 2. In the Uden2 simulation, one urea molecule makes a hydrogen bond with the carbonyl group of Ala37 and is involved in edge-to-face and face-to-face interactions with the indole ring of Trp35 before entering the core 2 in the final 100 ps. Once in the core, it interacts with the sidechains of Trp35, Leu42, and Ile51. Protein-engineering analysis of mutations at Ile25, Val45, Ile51, and Tyr78 indicates that the interactions made by these residues are broken early during unfolding [25], in agreement with the simulation results.

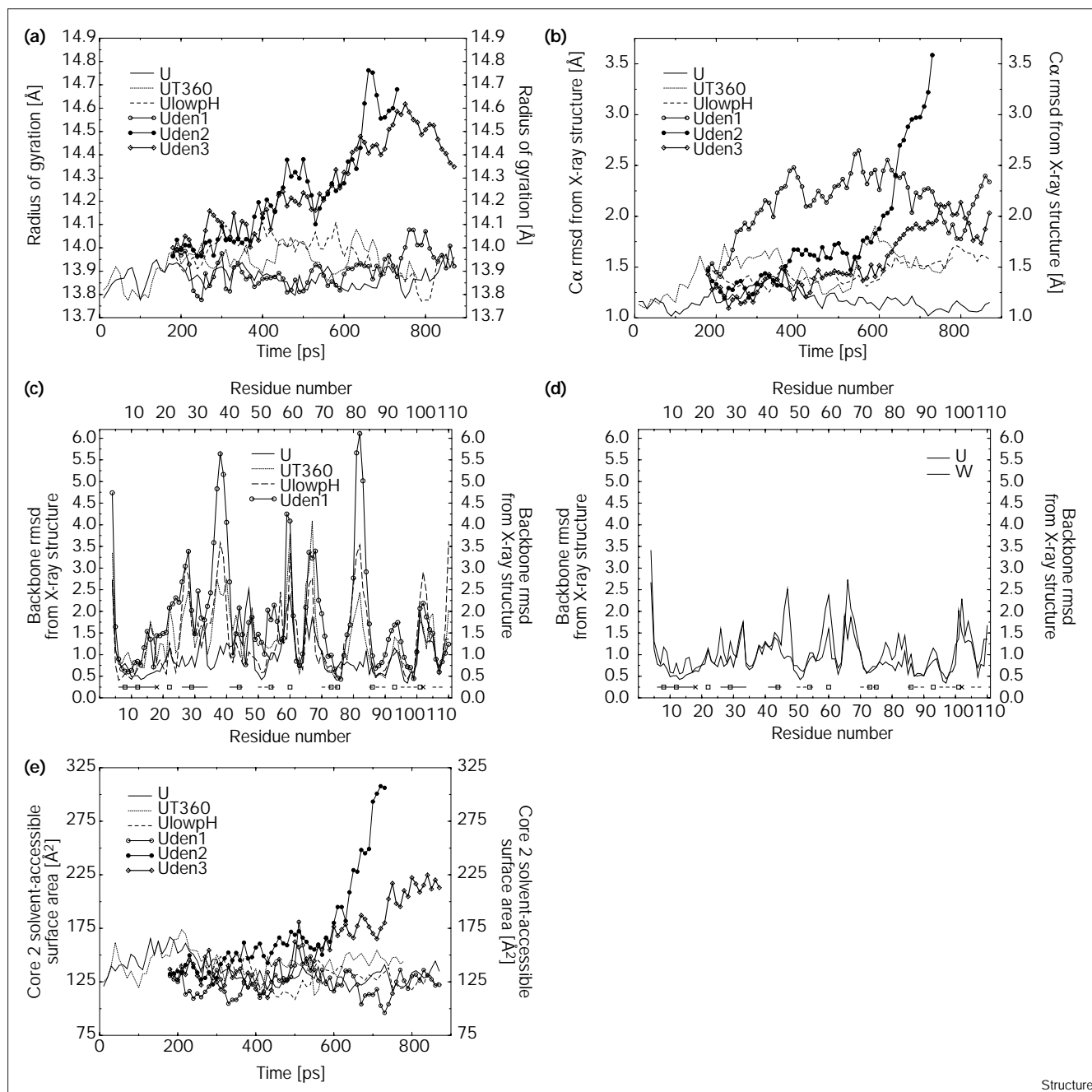
Cores 1 and 3 are compact and ‘dry’ throughout all of the simulations — there are neither water nor urea molecules in these cores (not shown).

In the simulations W and U the amount of exposed hydrophobic surface of barnase is essentially the same. During the last 200 ps, the apolar solvent-accessible surface was  $3072 \pm 57\text{ Å}^2$  in W and  $3105 \pm 43\text{ Å}^2$  in U, the accessible surface of the polar groups was  $1894 \pm 39\text{ Å}^2$  in W and  $1816 \pm 44\text{ Å}^2$  in U, whereas the accessible surface of the charged groups was  $1613 \pm 43\text{ Å}^2$  in W and  $1686 \pm 34\text{ Å}^2$  in U. This is at variance with previous simulation results where it was found that the exposed hydrophobic area is larger in the presence of urea than in pure water [19].

#### Urea–barnase interactions

Table 1 lists the number of urea and water molecules in the barnase solvation shells during the final 200 ps of each molecular dynamics run. The first shell contains many more urea molecules than the bulk region, although the initial distribution was essentially uniform. The water/urea ratio of the simulation system is 4.56 (3746/821), whereas the value of the first-shell water/urea ratio averaged over the final 200 ps is  $2.54 \pm 0.11$ ,  $2.66 \pm 0.16$ ,  $2.07 \pm 0.11$ ,  $2.73 \pm 0.28$ ,  $2.18 \pm 0.13$ , and  $2.12 \pm 0.17$ , for U, UT360, UlowpH, Uden1, Uden2, and Uden3, respectively. In the Uden simulations, the number of multiple hydrogen-bonded water molecules decreases, with little change in the multiple bonded urea molecules.

Figure 2



Structure

Global properties from simulations. (a) Radius of gyration ( $R_g$ ), (b) C $\alpha$  rmsd from the X-ray structure for amino acids 4–110. Solvent-accessible surface area of core 2. (c) Mainchain rmsd from the X-ray structure as a function of residue number. Values were averaged over the final 200 ps for simulations U, UT360, and UlowpH, and over the final 50 ps for Uden1. The X-ray structure does not determine the

positions of the N-terminal residues 1–3. At the bottom of the plot, the continuous segments represent  $\alpha$  helices, the broken segments  $\beta$ -sheet strands, the boxes Asp and Glu positions, and the crosses His positions. (d) Same as (c) for simulation W and U. (e) Solvent-accessible surface area of core 2. For parts (a), (b), and (e) the results shown are averaged over 10 ps time intervals.

To examine the nature of the urea solvation, we analyzed the hydrogen bonds between the protein and the urea molecules. In the final 200 ps, between 47% (UT360) and 51% (U, Uden2, and Uden3) of the urea molecules

in the first shell are involved in hydrogen bonds with polar or charged groups on the surface of barnase, and among these between 15% (UT360) and 18% (U) make multiple hydrogen bonds with barnase (Table 1). This is

Table 1

## Solvation-sphere statistics during final 200 ps.

Simulation	Number of urea molecules				Number of water molecules			
	Within 3 Å*	Within 6 Å	H bonded <sup>†‡</sup>	Multiple H bonded <sup>‡</sup>	Within 3 Å	Within 6 Å	H bonded <sup>‡</sup>	Multiple H bonded <sup>‡</sup>
W					489 (11)	1203 (20)	260 (7)	63 (5)
U	118 (4)	243 (6)	60 (5)	21 (4)	300 (7)	682 (13)	181 (7)	53 (5)
UT360	110 (4)	215 (6)	52 (6)	16 (4)	291 (10)	698 (18)	173 (8)	50 (5)
UlowpH	134 (5)	268 (8)	67 (5)	21 (4)	278 (8)	647 (16)	158 (5)	41 (4)
Uden1	113 (8)	226 (11)	55 (5)	18 (3)	306 (12)	721 (19)	166 (6)	35 (5)
Uden2	124 (5)	238 (6)	63 (6)	21 (4)	269 (9)	650 (11)	145 (6)	32 (4)
Uden3	129 (6)	249 (7)	66 (5)	22 (4)	273 (13)	655 (18)	149 (10)	31 (5)

Standard deviations are in parentheses. \*A urea or water molecule belongs to the first solvation shell if at least one atom is within 3.0 Å of any atom of barnase. <sup>†</sup>A maximal distance of 3.5 Å between donor and acceptor and a minimal angle of 120° between donor–H–acceptor were used.

<sup>‡</sup>Hydrogen bonded and multiple hydrogen bonded to barnase.

in disagreement with previous simulation results where it was found that almost all urea molecules in the first shell form at least one hydrogen bond with barnase [19]. The water hydrogen bonding to the protein in pure water and in urea is similar. In the pure water simulation (W) there are 53% of the first shell water molecules participating in hydrogen bonds with barnase while for the 8 M urea simulations this percentage varies from 54% (Uden1 and Uden2) to 60% (U).

Between 11% (Uden1 and Uden3) and 18% (U) of the first-shell water molecules are involved in multiple hydrogen bonds with barnase. Table 2 shows the hydrogen-bond statistics during the final 200 ps. Urea molecules donate about twice as many hydrogen bonds to barnase than they accept because of the 4/2 ratio of H atoms/O lone pairs in the urea molecule and the 2/1 ratio of barnase mainchain O lone pairs/NH amide groups. As expected, the solvent donor/solvent acceptor ratio is smaller in the simulation at low pH. For urea it varies from about 2.6 at neutral pH to about 1.8 at low pH, whereas for water it

varies from about 1.6 at neutral pH to about 0.9 at low pH, and it is 1.7 in the simulation with pure water (Table 2). The number of intrabarnase hydrogen bonds and the sum of urea–barnase, water–barnase, and intrabarnase hydrogen bonds are almost constant. The variance is even smaller if one considers the neutral and low pH simulations separately; for the former, the total number of hydrogen bonds ranges from 408 (UT360) to 433 (U), whereas for the latter it ranges from 364 (Uden2) to 389 (UlowpH). It is striking that during the final 200 ps of both simulations performed at 300K and neutral pH, namely W (pure water) and U (8 M urea), there are  $93 \pm 4$  intrabarnase hydrogen bonds and the total number of intrabarnase and solvent–barnase hydrogen bonds is approximately the same ( $430 \pm 9$  in W and  $433 \pm 9$  in U; Table 2).

The number of urea–barnase hydrogen bonds is plotted in Figure 3 as a function of the barnase  $R_g$  for the three Uden simulations. There is an increase from about 75 urea–barnase hydrogen bonds at  $R_g$  values of 13.6–13.8 Å to about 95 hydrogen bonds at  $R_g$  values of 14.6–14.8 Å for

Table 2

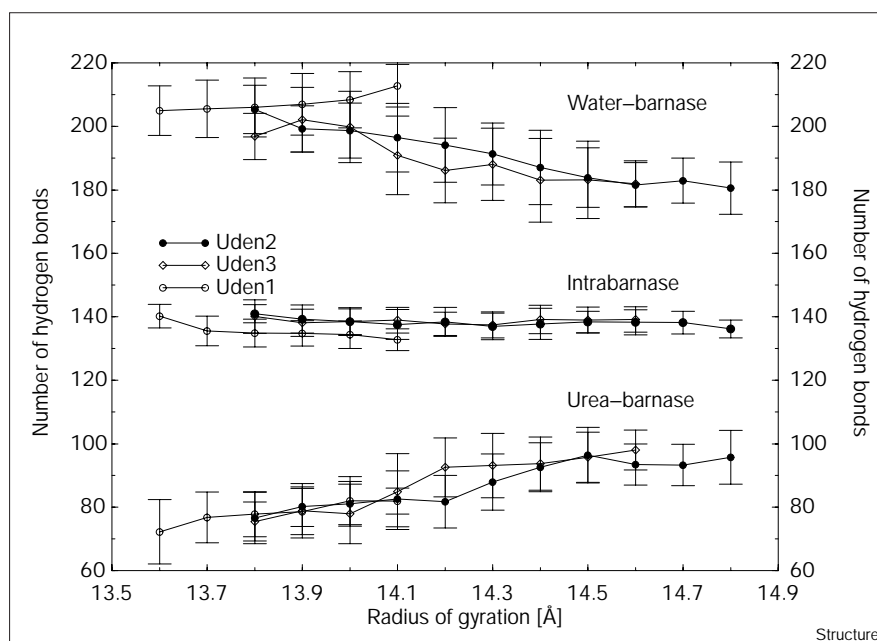
## Hydrogen-bond statistics during final 200 ps.

Simulation	Number of urea–barnase hydrogen bonds			Number of water–barnase hydrogen bonds			
	Total	Urea as acceptor	Urea as donor	Total	Water as acceptor	Water as donor	Intrabarnase
W				337 (9)	125 (5)	213 (6)	93 (4)
U	89 (9)	26 (4)	64 (7)	250 (12)	95 (6)	155 (9)	93 (4)
UT360	73 (9)	19 (4)	54 (8)	235 (11)	90 (6)	144 (9)	100 (4)
UlowpH	93 (8)	33 (3)	60 (7)	211 (8)	109 (4)	102 (6)	85 (4)
Uden1	79 (7)	28 (4)	50 (6)	209 (9)	109 (6)	100 (7)	84 (4)
Uden2	90 (10)	34 (6)	56 (6)	185 (8)	98 (6)	87 (5)	89 (4)
Uden3	93 (9)	32 (4)	61 (7)	186 (13)	100 (6)	86 (9)	89 (4)

Standard deviations are in parentheses. Same hydrogen-bond criterion as in Table 1.



Figure 3



Number of hydrogen bonds and standard deviation plotted as a function of  $R_g$ . Upper part: water–barnase, middle part: barnase, lower part: urea–barnase. A maximal distance of 3.5 Å between donor and acceptor and a minimal angle of 120° between donor–H–acceptor were used.

both the Uden2 and Uden3 simulations. The range of values of  $R_g$  in Uden1 is smaller (from 13.6 to 14.1 Å) but there is a similar increasing trend for the number of urea–barnase hydrogen bonds. The intrabarnase hydrogen bonds are almost unchanged whereas the number of water–barnase hydrogen bonds decreases from about 200 to about 180 in Uden2 and Uden3. Hence, the total number of hydrogen bonds is almost constant for  $R_g$  values in the 13.6–14.8 Å range, with urea–barnase hydrogen bonds replacing those with water.

Values of the nonbonding interaction energies per molecule of solvent or cosolvent are listed in Table 3. Only

the molecules in the first shell around the barnase surface are taken into account. The urea molecules interact more favorably by about 0.5 kcal/mol with nonpolar groups than the water molecules. Also, the total urea–barnase interaction energy is more favorable by about 1 kcal/mol than the water–barnase interaction energy. Moreover, the total interaction energy of a urea molecule in the first solvation shell of barnase (sum of urea–barnase, urea–urea and urea–water) is more favorable by about 2 kcal/mol than the total interaction energy of a urea molecule in an aqueous urea solution without barnase (sum of urea–urea and urea–water). On the other hand, a water molecule in the first solvation shell of

Table 3

Values of the nonbonding interactions per solvent molecule.

	Urea–barnase*						Water–barnase†									
	aliphatic	aromatic	polar	backbone	charged	total	urea–urea‡	urea–water‡	aliphatic	aromatic	polar	backbone	charged	total	water–urea§	water–water§
W									–0.1	–0.2	–0.7	–2.1	–3.6	–6.7		–9.7
U	–0.3	–0.5	–1.0	–3.5	–3.9	–9.1	–7.3	–6.1	–0.1	–0.2	–0.7	–2.2	–4.9	–8.2	–1.2	–6.2
UT360	–0.4	–0.6	–1.0	–3.1	–3.2	–8.4	–6.4	–6.2	–0.1	–0.2	–0.6	–2.2	–4.6	–7.7	–1.1	–5.9
							(–7.2)¶	(–13.5)¶							(–3.5)¶	(–10.9)¶

All values are in kcal/mol and represent averages over the final 200 ps for simulations W, U, and UT360. \*Urea or †water molecules with one or more atoms within 3 Å of any barnase atom (first shell) were considered in the evaluation of the energy. ‡Urea or water molecules with one or more atoms within 3 Å of a urea molecule in the first solvation shell of barnase were considered. §Urea or water molecules

with one or more atoms within 3 Å of a water molecule in the first shell of barnase were considered. ¶Values from a 110 ps simulation of an 8 M urea–water mixture in a sphere of 36 Å radius (without barnase). Averages were made over the final 50 ps and only for the urea and water molecules within 24 Å from the sphere center to avoid the boundary effects.

barnase improves its total interaction energy by about 1 kcal/mol with respect to a water molecule in an aqueous urea solution without barnase. These energy values are consistent with the aforementioned enrichment of urea molecules in the barnase solvation shell. The values of the energy contributions of the W and U simulations indicate that the urea molecules improve the capability of the water molecules to participate in hydrogen bonds with the charged groups of barnase, probably by promoting a more ordered water solvation shell around the charged sidechains. In fact, the interaction energy between first shell water molecules and charged groups improves from  $-3.6$  kcal/mol in pure water (simulation W) to  $-4.9$  kcal/mol in 8 M urea (simulation U, Table 3).

The simulation results for the interaction energies per molecule indicate that both models mentioned in the Introduction can contribute to denaturation — urea molecules interact favorably with protein polar groups [5] and urea can stabilize hydrophobic groups in water [7]. However, from the data for the simulations W and U it appears that the urea molecules do not increase the ‘adaptability’ of the water structure in the first solvation shell of the protein. In fact, the water–water interaction energy deteriorates from  $-9.7$  kcal/mol (simulation W) to  $-6.2$  kcal/mol (simulation U, Table 3).

#### Preferential binding sites

From the molecular dynamics trajectories the continuous residence times of the urea and water molecules were determined for all atoms of barnase. The continuous residence time for the urea molecule  $m$  in contact with the barnase atom  $a$  is defined as the simulation interval during which at least one atom of urea  $m$  remained within  $4 \text{ \AA}$  of the barnase atom  $a$ . It was necessary to augment the criterion of first-shell molecules by  $1 \text{ \AA}$  (from  $3\text{--}4 \text{ \AA}$ ) to neglect very short transient separations. Tables 4 and 5 list the urea molecules with long continuous residence time ( $\tau$ ) for the neutral-pH and low-pH simulations, respectively. All urea molecules with a  $\tau$  value greater than 150 ps for any atom in any simulation are listed; for example urea 388 occurs in both the U and UT360 simulations but has  $\tau > 150$  ps only in the U simulation. It is interesting to note that in spite of the large number of urea molecules that interact with barnase, only a very small number have long residence times even with a relatively generous threshold criterion for separation of  $4 \text{ \AA}$ . The rapid exchange behavior is in accord with NOE measurements [11]. The majority of these urea molecules are involved in hydrogen bonds with polar groups of barnase and are in pockets or crevices (Figures 4a–c). Some of the preferential binding sites are common to both the neutral- and low-pH runs; the equivalent numbers are given in a footnote to Table 5. However, in the neutral-pH simulations (U and UT360) urea878 is trapped in loop 4 by hydrogen bonds with the mainchain

**Table 4**

**Urea molecules with long continuous residence time  $\tau$  in the neutral pH simulations U or UT360.**

Urea no.	Residue	Atom	U $\tau$ (ps)	UT360 $\tau$ (ps)
878*	Asn77	O	258	90
878	Tyr78	HA	700	255
878	Tyr78	HD1	390	68
878	Tyr78	HE1	279	37
878	Thr79	HN	700	254
878	Thr79	N	320	243
878	Thr79	HB	318	143
878	Ser80	HN	373	249
878	Ser80	N	319	74
878	Ser80	O	326	155
878	Ser80	C	283	58
878	Phe82	O	273	91
878	Asn84	HD21	207	93
539	Lys19	HA	191	64
539	Arg72	HD2	209	60
539	Tyr90	HE1	614	195
539	Tyr90	HE1	614	195
539	Tyr90	CE1	287	112
539	Tyr90	CZ	310	110
539	Tyr90	HH	619	174
539	Tyr90	OH	617	140
539	Trp94	HH2	344	107
350	Ser67	HA	173	128
350	Gly68	HN	399	280
350	Gly68	N	259	126
350	Arg69	HN	168	133
350	Arg69	O	169	84
607	Ile55	O	164	312
607	Phe56	HD1	296	283
607	Phe56	HA	238	299
607	Glu73	HG2	238	216
607	Glu73	CG	197	119
607	Glu73	CD	198	386
607	Glu73	OE1	152	129
607	Glu73	OE2	267	298
607	Tyr103	HH	277	399
607	Tyr103	OH	73	381
388	Ser85	HB1	226	28
388	Asp101	HA	600	64
388	His102	HN	345	116
388	His102	HB2	210	71
413	Thr105	HA	202	42
413	Thr105	HG22	286	28
413	Phe106	HN	593	41
413	Phe106	N	399	30
413	Phe106	HB2	418	93
514*	Ala1	HN3	284	84
514	Ala1	N	265	121
514	Ala1	HB3	293	53
514	Asn5	HD22	590	14
514	Asn77	HA	233	221
514	Asn77	OD1	159	89
514	Tyr78	O	168	50
514	Thr79	OG1	220	118
915	Asn41	HA	116	286
915	Ala43	HN	40	153
915	Asp44	HB2	249	259
828	Ser92	HA	35	473
828	Trp94	CE2	31	178

For a given urea molecule all barnase atoms with a continuous residence time of 150 ps or more are listed. Atoms of polar groups are in *italics*. \*Urea molecules 878 and 514 are shown in Figure 4b.

Table 5

Urea molecules with long continuous residence time ( $\tau$ ) in the low-pH simulations.

Urea number*	Residue	Atom	UlowpH $\tau$ (ps)	Uden1 $\tau$ (ps)	Uden2 $\tau$ (ps)	Uden3 $\tau$ (ps)	Average Uden1–3 (ps)
142 <sup>†</sup>	Thr70	OG1	321	87	123	140	117
142	Arg72	HG1	561	360	118	166	215
142	Arg72	HD2	699	184	253	103	180
142	Tyr90	HD1	307	323	272	185	260
142	Ser91	HA	317	181	52	70	101
142	Ser91	O	280	514	292	185	330
142	Ser91	C	419	514	187	144	282
142	Ser92	N	673	501	210	144	285
142	Ser92	HA	700	599	555	186	447
562 <sup>†</sup>	Tyr90	HE1	700	700	193	107	333
562	Tyr90	HH	700	700	244	121	355
562	Tyr90	OH	661	700	104	107	304
562	Trp94	HH2	387	218	93	79	130
530 <sup>†</sup>	Leu20	HN	700	397	99	140	212
530	Leu20	N	550	151	62	101	105
530	Leu20	HB2	598	183	133	171	162
530	Lys19	HA	373	254	74	132	153
530	Lys19	HB1	450	95	86	51	77
667	Asp54	HB1	279	394	55	100	183
667	Ile55	O	458	132	133	102	122
667	Phe56	HA	495	177	138	129	148
667	Glu73	HG1	454	41	105	9	52
667	Glu73	HG2	483	94	232	31	119
667	Glu73	CG	483	67	112	12	64
667	Glu73	CD	540	55	116	75	82
667	Glu73	HE2	686	85	216	75	125
667	Glu73	OE2	686	85	220	70	125
226	Thr6	HA	161	202	158	308	223
226	Thr6	HB	201	217	117	244	193
226	Phe7	HN	296	208	189	308	235
226	Phe7	HD1	228	222	184	341	249
226	Phe7	CD1	184	80	167	232	160
226	Asn77	HD22	330	186	68	162	139
607	Asn58	O	587	172	84	126	127
607	Asn58	C	584	33	41	39	38
607	Asn58	HA	584	76	19	152	82
607	Arg59	HB2	641	66	62	82	70
607	Glu60	CD	394	44	64	116	75
607	Glu60	OE1	432	72	32	133	79

For a given urea molecule all barnase atoms with a continuous residence time of 150 ps or more are listed. Atoms of polar groups are in *italics*. \*The urea molecules that are equivalent to those in Table 4 are: 562→539 and 667→607. <sup>†</sup>Urea molecules 142, 562 and 530 are shown in Figure 4c.

carbonyl oxygens of Asn77, Ser80, and Phe82 and the mainchain NH of Thr79 and Ser80 (Table 4 and Figure 4b). Loop 4 is not a preferential binding site for urea in the low-pH simulations, probably because of the protonation of the Asp75 and Asp86 sidechains, which are relatively close to the urea-binding site.

Urea and water molecules have significantly shorter residence times at 360K than at 300K. For most of the stably bound urea molecules the ratio of the residence time at 300K over the residence time at 360K varies between 1.5 and 3. From these values, one obtains an estimate of 1.5 kcal/mol to 4.0 kcal/mol for the activation energy of

urea dissociation. These values can be compared with simulation estimates of the activation energy for breaking water–lysozyme hydrogen bonds of 1.1–1.4 kcal/mol (M Buck and MK, unpublished results).

In the low-pH simulations, urea142 participates in interactions with polar groups of the mainchain and with the OH group of Thr70 (Table 5 and Figure 4c). It is almost completely buried in a deep pocket for most of the trajectories and interacts with the aromatic rings of Tyr90 and Trp94.

The hydroxyl group of Tyr90 is at the bottom of a pocket formed by the sidechains of Trp94 and Arg72 (Figure 4c).



**Figure 4**

Stereo pictures of some of the urea molecules with very long continuous residence time on the surface of barnase. Atoms and dotted Connolly surfaces are colored according to element type: white for carbons, blue for nitrogens, red for oxygens, and cyan for hydrogens. Water molecules are shown as small red spheres. (a) Simulation U at 500 ps. Urea molecules with long residence time are in a CPK rendering. (b) Simulation U at 162.5 ps. Urea878 and urea514 are in ball-and-stick representation and hydrogen bonds are shown as green dashed lines. Other urea molecules are shown in a stick representation without hydrogens. (c) Simulation UlowpH at 500 ps. Urea142, urea 562, and urea530 are in ball-and-stick representation and hydrogen bonds are shown as green dashed lines. Other urea molecules are shown in a stick representation without hydrogens.

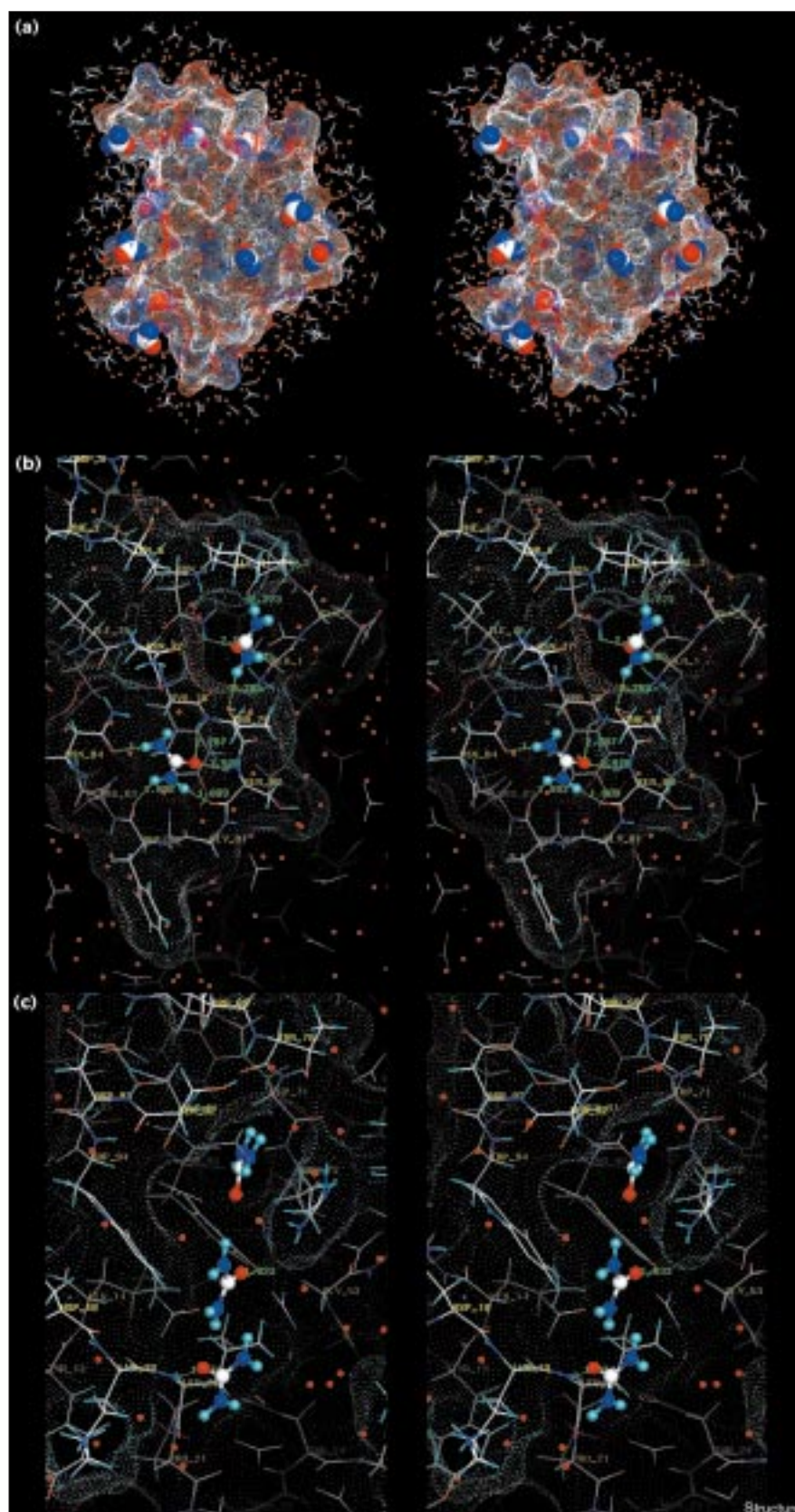


Table 6

## Simulations performed\*.

	Started from	Temperature (K)	Length		
			pH	(ps)	Name
Control run	Crystal	300	neutral	700	W
Urea	Crystal	300	neutral	870	U
Urea high T	Crystal	360	neutral	780	UT360
Urea low pH	170 ps UT360	300	low	700	UlowpH
Urea high T, low pH	170 ps UT360	360	low	700	Uden1
Urea high T, low pH	170 ps UT360	360	low	555	Uden2
Urea high T, low pH	170 ps UT360	360	low	700	Uden3

\*All simulations were performed in 8 M urea solution apart from the control run (W), which was performed in pure water.

This is a preferential binding site for urea in all of the simulations and the hydrogen bond between the urea oxygen and the OH of Tyr90 is almost always present (Tables 4 and 5).

Most of the mainchain preferential binding sites (see Supplementary material) are in loops or in terminal turns of the  $\alpha$  helices because the NH and CO groups of these regions are less buried than the ones in the  $\beta$  sheet and in the central turns of the  $\alpha$  helices. Some backbone polar groups interact with urea at both neutral and low pH (20HN,  $\tau = 246$  ps in simulation U and  $\tau = 700$  ps in UlowpH; 58CO,  $\tau = 238$  ps in U and  $\tau = 587$  ps in UlowpH) but there are also some polar groups that form preferential binding sites only at neutral pH (79HN,  $\tau = 700$  in U and  $\tau = 21$  ps in UlowpH) or low pH (92HN,  $\tau = 1$  ps in U and  $\tau = 329$  ps in UlowpH). The different behavior for the latter might depend on the protonation state of Asp93, whose sidechain is close to 92HN. On average there are more urea molecules interacting with mainchain CO than with NH groups. This is consistent with experimental findings on the greater solubilizing effect of guanidinium chloride than urea on ATGEE [5]; the guanidinium group, which has three  $\text{NH}_2$  groups, can interact in any orientation with the protein CO groups. The results in Tables 4, 5, and in the supplementary material suggest that at least some of the urea-protein interactions last long enough to be accessible by NMR, in analogy with the studies on the small proteins BPTI and PEC-60 [11].

The testing of the simulation data presented here provides a challenge for experimentalists. Of particular interest would be more data on specific binding sites in barnase from NMR and X-ray studies in the presence of urea.

## Discussion

There is a substantial increase in the number of urea molecules in the first solvation shell around the surface of barnase. Guanidinium chloride and urea have been shown to increase the surface tension of water and also to act as 'salting-in' agents for a solute like benzene (they increase the solubility of benzene in water) [26,27]. This has been

interpreted to mean that the salting-in properties of these cosolvents originate from direct interactions between urea (or guanidinium chloride) and the solute and not from easier cavity formation in water. Such direct interactions reflect an increase in the number of urea molecules in the solvation sphere. A significant increase in the urea/water ratio in the first shell has also been observed in a very recent molecular dynamics simulations of the unfolding of barnase in the presence of urea, performed with a different force field and different boundary conditions [19].

An analysis of the urea molecules in the barnase solvation shell demonstrated that about one half are involved in hydrogen bonds with barnase. The other half are in contact with apolar groups on the protein surface and/or participate in hydrogen bonds with water and/or other urea molecules. This is at variance with the results of Tirado-Rives *et al.* who stated that almost all of the first-shell molecules of urea (87 of 91 at 298K) were involved in hydrogen bonds with barnase [19]. This discrepancy may be a consequence of the less restrictive criterion for hydrogen bonding used by them — they did not use an angle criterion whereas a minimal angle of  $120^\circ$  between donor-H-acceptor was employed in our study.

The amount of apolar and polar solvent-accessible surface is essentially the same in the simulations with and without urea. This disagrees with the results of Tirado-Rives *et al.* who stated that in the presence of urea the solvent-accessible surface of the hydrophobic regions is larger than in pure water [19].

Most of the urea molecules with long residence time are in pockets or crevices on the barnase surface. Furthermore, there is no replacement of intra-protein interactions with urea molecules in the folded structure. This is in agreement with the NOE measurements for BPTI and PEC-60 at urea concentrations of up to 8 M [11].

The preferential binding sites on the protein mainchain are not evenly distributed between regular and non-

regular secondary structure. There is a greater likelihood of finding urea molecules associated with loops and terminal regions of helices, namely regions with one or more exposed mainchain polar groups.

## Biological implications

The understanding of protein folding and unfolding is an essential aspect of protein chemistry. This is of ever increasing importance because of the realization that a number of diseases, such as Alzheimer's disease [28] and bovine spongiform encephalopathy [29], are likely to result from protein misfolding. Although urea is not known to be involved in unfolding in the cell, it is such a useful tool for protein-folding studies that a detailed description of the molecular mechanism of urea unfolding is an important element in interpreting the experimental data.

A series of simulations of barnase with explicit aqueous solvent and in the presence of urea have been performed to elucidate the structural and energetic basis of the interactions of urea with proteins. At the same time, information was obtained on how the presence of urea affects the water-protein interactions. Both of these are important for understanding the mechanism of protein denaturation by urea.

The urea molecules are found to interact with both polar and nonpolar groups on the surface of barnase. Moreover, the presence of urea improves the capability of water molecules to participate in hydrogen bonds with hydrophilic groups of barnase. The energetic analysis indicates that in an aqueous urea solution both the hydrophilic and the hydrophobic regions of the protein chain are solvated more favorably than in a pure water solution. Our results therefore support both models of urea stabilization of the unfolded protein conformation; namely, there are direct interactions of urea molecules with functional groups at the protein surface and the aqueous urea solution around nonpolar amino acid sidechains provides better solvation than pure water. This is in agreement with solubility measurements of ATGEE, a model system that is representative of the protein mainchain, and solubility measurements of polar and nonpolar amino acids in aqueous urea solution. Moreover, as remarked recently by Tsai *et al.*, each urea molecule in the first solvation shell reduces the entropic penalty of binding because it replaces three of the first-shell water molecules. According to these arguments, the urea molecules stabilize both the native and unfolded protein conformations, but the larger number of exposed functional groups in the latter favors denaturation.

## Materials and methods

The all-hydrogen (CHARMM22) parameter set [30] and the CHARMM program [31] were used for the simulations and the modified TIP3P model was employed for the water molecules [23,32]. Hydrogen atoms were added to the coordinates of the X-ray crystal structure of barnase

by the HBUILD option [33] of the CHARMM program [31]. To reproduce low-pH conditions, the acidic residues were neutralized by adding a hydrogen atom to one of the two sidechain oxygen atoms [18]. This was done for all Asp and Glu residues apart from Asp93 whose pKa is lowered in the native state to below 1 because of the ionic interaction with Arg69 [34,35]. The pKa value of His18 and His102 are 7.9 and 6.3, respectively [36]. Hence, the two His sidechains were charged in the low-pH simulations whereas in the neutral pH simulations His18 was charged and His102 was neutral with a proton on N $\delta$ . This yields total charges of +16 and +3 electronic charges at low and neutral pH, respectively. Parameters for the urea atoms were derived in analogy with the amide of the Asn and Gln sidechains. The partial charges of -0.51 (O), 0.51 (C), -0.62 (N), 0.31 (H) are close to those used by Levitt and coworkers in the ENCAD force field: -0.38 (O), 0.38 (C), -0.666 (N), 0.333 (H) [12].

For the preparation of the urea/water mixture, 118 urea molecules were first randomly distributed on a sphere of 18 Å radius. They were then immersed in a previously equilibrated 18 Å sphere of 796 water molecules and all water molecules overlapping with the urea molecules were deleted. This yielded an 18 Å sphere of 118 urea and 522 water molecules, which was equilibrated for 10 ps of Langevin dynamics at 300K. A box of 15 Å size was then cut out of the equilibrated sphere and replicated along the x, y, and z directions to form a sphere of 36 Å radius with 4168 water molecules and 915 urea molecules corresponding to an 8 M urea concentration at a density of 1.120 g/cm<sup>3</sup>. This system was first equilibrated for 2 ps of Langevin dynamics at 300K. The X-ray crystal structure of barnase supplemented by the hydrogen atoms was then immersed in the equilibrated sphere and water and urea molecules overlapping with barnase atoms were deleted. The criterion for overlapping was a distance smaller than 2.7 Å between the water oxygen and any heavy atom of barnase, and a distance of less than 2.4 Å between any heavy atom of urea and barnase. The final molecular system consisted of barnase (1728 and 1741 atoms at neutral and low pH, respectively) centered in a sphere of 36 Å radius with 3746 water and 821 urea molecules. Atoms in a spherical region of 32 Å radius were treated by Newtonian dynamics, whereas the solvent and denaturant molecules in the spherical shell from 32 to 36 Å were treated by Langevin dynamics with a deformable boundary potential [37]. The leap-frog integrator was used in all runs with an integration step of 2 fs and the nonbonding pair list was updated every 20 steps. The CHARMM22 default cutoffs for long range interactions were used, i.e., a shift function was used for the electrostatic term with cutoff at 12 Å, and a switch truncation acting between 10 and 12 Å was employed for the van der Waals interaction [30]. Structures were saved every 0.5 ps. The solvent-accessible surface area was calculated with an analytical method implemented in CHARMM using a probe sphere of 1.4 Å radius.

Table 6 lists the simulations that were performed. In previous denaturation simulations in pure water (with the CHARMM polar-hydrogen force field [23]), it had been found that at low pH barnase was stable for at least 300 ps at 300K, whereas it began to denature in less than 100 ps at 360K [18].

## Supplementary material

Supplementary material available with the Internet version of this paper contains a table listing the backbone polar groups with continuous urea residence time ( $\tau$ ) larger than 100 ps in U or UlowpH.

## Note added in proof

A recent study [38] of the energetics of dissolution of cyclic peptides in aqueous urea solutions supports the conclusions of our paper.

## Acknowledgements

This work was supported by the Swiss National Science Foundation (grant number 31-53604.98) and by the United States National Science Foundation. AC thanks A Tissot for interesting and helpful discussions. We thank A Widmer (Novartis Pharma Inc., Basel) for the molecular modeling program WITNOTP, which was used for visual analysis of the trajectories and for



preparing Figures 4a–c. The atomic coordinates of barnase were kindly provided by A Cameron and G Dodson of the University of York. The simulations were performed on an SGI Power Challenge at the Computer Center of the University of Zürich from January 1996 until August 1997.

## References

1. Tanford, C. (1970). Protein denaturation. C. Theoretical models for the mechanism of denaturation. *Adv. Protein Chem.* **24**, 1-95.
2. Pace, C.N. (1986). \newblock Determination and analysis of urea and guanidine hydrochloride denaturation curves. *Methods Enzymol.* **131**, 266-280.
3. Schellman, J.A. (1987). Selective binding and solvent denaturation. *Biopolymers* **26**, 549-559.
4. Myers, J.K., Pace, C.N. & Scholtz, J.M. (1995). Denaturant m values and heat capacity changes: relation to changes in accessible surface areas of protein unfolding. *Protein Sci.* **4**, 2138-2148.
5. Robinson, D.R. & Jencks, W.P. (1965). The effect of compounds of the urea-guanidinium class on the activity coefficient of acetyltetraglycine ethyl ester and related compounds. *J. Am. Chem. Soc.* **87**, 2462-2470.
6. Makhatadze, G.I. & Privalov, P.L. (1992). Protein interactions with urea and guanidinium chloride. a calorimetric study. *J. Mol. Biol.* **226**, 491-505.
7. Whitney, P.L. & Tanford, C. (1962). Solubility of amino acids in aqueous urea solutions and its implications for the denaturation of proteins by urea. *J. Biol. Chem.* **237**, PC1735-PC1737.
8. Nozaki, Y. & Tanford, C. (1963). The solubility of amino acids and related compounds in aqueous urea solutions. *J. Biol. Chem.* **238**, 4074-4081.
9. Thayer, M.M., Haltiwanger, R.C., Allured, V.S., Gill, S.C. & Gill, S.J. (1993). Peptide-urea interactions as observed in diketopiperazine-urea cocrystal. *Biophys. Chem.* **46**, 165-169.
10. Pike, A.C.W. & Acharya, K.R. (1994). A structural basis for the interaction of urea with lysozyme. *Protein Sci.* **3**, 706-710.
11. Liepinsh, E. & Otting, G. (1994). Specificity of urea binding to proteins. *J. Am. Chem. Soc.* **116**, 9670-9674.
12. Tsai, J., Gerstein, M. & Levitt, M. (1996). Keeping the shape but changing the charges: A simulation study of urea and its iso-steric analogs. *J. Chem. Phys.* **104**, 9417-9430.
13. Mauguen, Y., *et al.* & Jack, A. (1982). Molecular structure of a new family of ribonuclease. *Nature* **297**, 162-164.
14. Baudet, S. & Janin, J. (1991). Crystal structure of a barnase-d(GpC) complex at 1.9 Å resolution. *J. Mol. Biol.* **219**, 123-132.
15. Bycroft, M., Ludvigsen, S., Fersht, A.R. & Poulsen, F.M. (1991). Determination of the three-dimensional solution structure of barnase using nuclear magnetic resonance spectroscopy. *Biochemistry* **30**, 8697-8701.
16. Fersht, A.R. (1993). Protein folding and stability: the pathway of folding of barnase. *FEBS Lett.* **325**, 5-16.
17. Fersht, A.R. (1994). Pathway and stability of protein folding. *Biochem. Soc. Trans.* **22**, 267-273.
18. Caffisch, A. & Karplus, M. (1995). Acid and thermal denaturation of barnase investigated by molecular dynamics simulations. *J. Mol. Biol.* **252**, 672-708.
19. Tirado-Rives, J., Orozco, M. & Jorgensen, W.L. (1997). Molecular dynamics simulations of the unfolding of barnase in water and 8 M aqueous urea. *Biochemistry* **36**, 7313-7329.
20. A. Matouschek, J.M. Matthews, C.M. Johnson & A.R. Fersht. (1994). Extrapolation to water of kinetic and equilibrium data for the unfolding of barnase in urea solutions. *Protein Eng.* **7**, 1089-1095.
21. Johnson, C.M. & Fersht, A.R. (1995). Protein stability as a function of denaturant concentration: The thermal stability of barnase in the presence of urea. *Biochemistry* **34**, 6795-6804.
22. Serrano, L., Matouschek, A. & Fersht, A.R. (1992). The folding of an enzyme. III. Structure of the transition state for unfolding of barnase analysed by a protein engineering procedure. *J. Mol. Biol.* **224**, 805-818.
23. Neria, E., Fischer, S. & Karplus, M. (1996). Simulation of activation free energies in molecular systems. *J. Chem. Phys.* **105**, 1902-1921.
24. Caffisch, A. & Karplus, M. (1994). Molecular dynamics simulation of protein denaturation: Solvation of the hydrophobic cores and secondary structure of barnase. *Proc. Natl Acad. Sci. USA* **91**, 1746-1750.
25. Matouschek, A., Serrano, L. & Fersht, A.R. (1992). The folding of an enzyme. IV. Structure of an intermediate in the refolding of barnase analysed by a protein engineering procedure. *J. Mol. Biol.* **224**, 819-835.
26. Breslow, R. & Guo, T. (1990). Surface tension measurements show that chaotropic salting-in denaturants are not just water-structure breakers. *Proc. Natl Acad. Sci. USA* **87**, 167-169.
27. Siskova, M., Hejtamankova, J. & Bartovska, L. (1985). Physicochemical properties of the ternary system urea, ammonium nitrate, water surface tension. *Collect. Czech. Chem. Commun.* **50**, 1629-1635.
28. Kelly, J.W. (1998). \newblock The alternative conformations of amyloidogenic proteins and their multi-step assembly pathways. *Curr. Opin. Struct. Biol.* **8**, 101-106.
29. Prusiner, S.B. (1997). Prion diseases and the BSE crisis. *Science* **278**, 245-251.
30. MacKerell, A.D., Jr. *et al.*, & Karplus, M. (1998). All-atom empirical potential for molecular modeling and dynamics studies of proteins. *J. Phys. Chem. B* **102**, 3586-3616.
31. Brooks, B.R., Bruccoleri, R.E., Olafson, B.D., States, D.J., Swaminathan, S. & Karplus, M. (1983). CHARMM: A program for macromolecular energy, minimization, and dynamics calculations. *J. Comput. Chem.* **4**, 187-217.
32. Jorgensen, W.L., Chandrasekhar, J., Madura, J., Impey, R.W., & Klein, M.L. (1983). Comparison of simple potential functions for simulating liquid water. *J. Chem. Phys.* **79**, 926-935.
33. Brünger, A. & Karplus, M. (1988). Polar hydrogen positions in proteins: empirical energy placement and neutron diffraction comparison. *Proteins* **4**, 148-156.
34. Oliveberg, M., Arcus, V.L. & Fersht, A.R. (1995). pKa values of carboxyl groups in the native and denatured states of barnase: the pKa values of the denatured state are on average 0.4 units lower than those of model compounds. *Biochemistry* **34**, 9424-9433.
35. Oliveberg, M. & Fersht, A.R. (1996). New approach to the study of transient protein conformations: the formation of a semiburied salt link in the folding pathway of barnase. *Biochemistry* **35**, 6795-6805.
36. Sali, D., Bycroft, M. & Fersht, A.R. (1988). Stabilization of protein structure by interaction of  $\alpha$ -helix dipole with a charged sidechain. *Nature* **335**, 496-500.
37. Brooks, C.L., III. & Karplus, M. (1989). Solvent effects on protein motion and protein effects on solvent motion. *J. Mol. Biol.* **208**, 159-181.
38. Zou, Q., Habermann, S.H.E. & Murthy, K.P. (1998). Urea effects on protein stability: hydrogen bonding and the hydrophobic effect. *Proteins* **31**, 107-115.
39. Kraulis, P. (1991). Molscript, a program to produce both detailed and schematic plots of protein structures. *J. Appl. Crystallogr.* **24**, 946-950.

---

Because *Structure with Folding & Design* operates a 'Continuous Publication System' for Research Papers, this paper has been published on the internet before being printed (accessed from <http://biomednet.com/cbiology/str>). For further information, see the explanation on the contents page.

# Supplementary material

## Structural details of urea binding to barnase: a molecular dynamics analysis

Amedeo Caflisch and Martin Karplus

Table S1

Backbone polar groups with continuous urea residence time ( $\tau$ ) larger than 100 ps in U or UlowpH.

Protein region	Atom name	U				UlowPh			
		< N >*	SD	Nv†	[PS]	< N >*	SD	Nv†	[PS]
N terminus	1O	1.80	(0.82)	21	153	2.37	(1.26)	23	79
N terminus	2O	1.78	(0.90)	23	86	2.31	(0.97)	24	197
N terminus	3O	0.91	(0.40)	5	68	0.79	(0.53)	4	330
N terminus	4HN	1.30	(0.88)	17	291	1.65	(1.04)	20	355
N terminus	4O	0.25	(0.43)	7	18	0.65	(0.55)	9	176
$\alpha$ 1	7HN	0.60	(0.58)	7	132	0.66	(0.57)	9	296
$\alpha$ 1	9O	0.50	(0.53)	5	172	1.12	(0.53)	8	94
$\alpha$ 1	13HN	0.40	(0.49)	4	169	0.69	(0.52)	4	56
$\alpha$ 1	15O	1.13	(0.65)	14	108	1.21	(0.74)	18	120
$\alpha$ 1	16O	0.88	(0.66)	15	57	2.40	(1.08)	20	120
$\alpha$ 1	17O	1.17	(0.84)	15	287	1.70	(0.84)	17	103
$\alpha$ 1	18O	2.02	(0.88)	15	100	1.68	(0.78)	15	158
loop 1	20HN	2.46	(0.81)	12	246	2.99	(0.91)	10	700
loop 1	20O	1.26	(0.69)	8	146	2.42	(0.65)	10	364
loop 1	21O	0.81	(0.68)	6	231	1.25	(0.56)	6	370
loop 1	24HN	0.45	(0.50)	3	183	0.82	(0.39)	2	112
loop 1	24O	1.42	(0.72)	9	119	1.60	(0.58)	8	157
$\alpha$ 2	27HN	0.07	(0.25)	1	9	0.61	(0.50)	5	220
$\alpha$ 2	28HN	0.21	(0.41)	5	24	0.79	(0.58)	11	222
$\alpha$ 2	29O	0.90	(0.56)	10	125	0.50	(0.53)	8	38
$\alpha$ 2	31O	1.48	(0.83)	20	76	1.86	(0.76)	25	160
$\alpha$ 2	32O	2.47	(1.01)	32	104	2.67	(0.99)	28	99
$\alpha$ 2	33O	2.08	(1.01)	21	157	2.00	(1.01)	25	82
loop 2	35O	1.22	(0.80)	11	138	2.02	(0.41)	7	345
loop 2	37HN	1.50	(0.68)	14	334	1.28	(0.77)	14	314
loop 2	37O	0.64	(0.70)	8	41	1.45	(0.87)	16	175
loop 2	38HN	0.92	(0.81)	22	116	0.71	(0.67)	17	48
loop 2	39O	1.30	(0.76)	12	140	2.81	(0.98)	17	152
$\alpha$ 3	43O	1.14	(0.77)	12	120	0.93	(0.83)	14	80
$\alpha$ 3	44O	0.80	(0.77)	15	105	2.01	(0.77)	19	126
$\alpha$ 3	45O	0.91	(0.78)	14	113	1.45	(0.81)	15	56
$\beta$ 1	55HN	0.64	(0.63)	11	115	0.92	(0.68)	9	109
$\beta$ 1	55O	1.92	(0.81)	15	164	1.74	(0.74)	11	458
loop 3	57HN	1.34	(0.94)	12	140	1.05	(0.81)	9	36
loop 3	57O	1.12	(0.57)	11	319	1.28	(0.72)	8	231
loop 3	58HN	0.25	(0.44)	4	86	1.57	(0.87)	17	122
loop 3	58O	1.49	(0.79)	14	238	1.27	(0.48)	5	587
loop 3	59O	1.99	(1.13)	24	107	2.47	(1.00)	23	249
loop 3	60O	1.20	(0.63)	14	172	2.37	(1.22)	25	137
loop 3	61O	1.86	(0.81)	22	81	2.64	(0.74)	17	202
loop 3	62O	1.40	(0.70)	13	73	2.13	(0.87)	12	207
loop 3	63O	1.72	(0.59)	11	170	1.33	(0.59)	9	343
loop 3	65HN	2.18	(1.04)	22	244	2.13	(1.15)	16	311
loop 3	66HN	1.04	(0.70)	11	111	0.86	(0.76)	10	67
loop 3	66O	1.70	(0.82)	14	125	1.80	(0.84)	23	104
loop 3	67O	1.61	(0.92)	26	124	2.50	(1.03)	25	194
loop 3	68HN	2.39	(0.84)	24	399	2.56	(1.07)	28	255
loop 3	68O	2.02	(0.92)	23	158	2.41	(0.96)	34	120
loop 3	69HN	1.69	(0.80)	14	168	1.52	(0.71)	20	275



Table S1 (continued)

$\beta$ 2	70HN	1.16	(0.73)	10	110	1.05	(0.75)	16	114
$\beta$ 2	70O	0.00	(0.04)	1	1	0.79	(0.45)	5	207
$\beta$ 2	71HN	0.41	(0.51)	3	136	0.83	(0.73)	9	80
$\beta$ 2	72HN	0.00	(0.00)	0	0	0.91	(0.33)	2	181
loop 4	77O	1.95	(0.81)	13	258	0.50	(0.57)	12	36
loop 4	78O	1.34	(0.58)	4	168	0.15	(0.36)	1	58
loop 4	79HN	1.81	(0.70)	10	700	0.26	(0.47)	7	21
loop 4	79O	0.68	(0.59)	7	114	0.23	(0.51)	4	44
loop 4	80HN	1.74	(0.81)	13	373	0.62	(0.61)	12	62
loop 4	80O	2.16	(0.91)	17	326	1.18	(0.85)	23	75
loop 4	81O	0.21	(0.42)	5	6	0.81	(0.67)	12	101
loop 4	82HN	1.74	(0.78)	15	206	1.67	(1.05)	23	122
loop 4	82O	2.24	(0.65)	10	273	1.05	(0.08)	12	143
loop 4	83HN	1.17	(0.63)	11	146	1.46	(0.73)	19	147
loop 4	83O	2.37	(0.62)	13	109	1.72	(0.63)	17	195
$\beta$ 3	90O	0.00	(0.00)	0	0	0.97	(0.20)	2	197
$\beta$ turn	91O	0.00	(0.05)	2	1	1.42	(0.50)	4	280
$\beta$ turn	92HN	0.00	(0.04)	1	1	1.05	(0.35)	5	329
$\beta$ turn	92O	0.84	(0.63)	18	80	2.32	(1.02)	18	231
$\beta$ turn	93O	1.47	(0.73)	11	102	1.72	(0.69)	12	164
$\beta$ turn	94O	0.77	(0.50)	2	111	1.08	(0.95)	10	265
$\beta$ 4	96HN	0.07	(0.26)	5	15	0.53	(0.63)	6	149
$\beta$ 4	100O	1.10	(0.49)	6	107	0.08	(0.29)	7	4
$\beta$ turn	102HN	1.76	(0.76)	13	345	1.17	(0.64)	15	165
$\beta$ turn	102O	0.95	(0.96)	15	76	1.16	(0.81)	11	135
$\beta$ turn	103O	0.51	(0.54)	9	33	1.97	(0.86)	13	436
$\beta$ turn	104O	1.46	(0.93)	12	104	0.96	(0.77)	12	43
C terminus	106HN	1.83	(0.83)	13	593	0.74	(0.86)	11	70
C terminus	106O	2.51	(0.67)	11	216	1.66	(1.05)	17	191
C terminus	108HN	1.77	(0.88)	17	282	1.27	(0.59)	15	247
C terminus	109O	1.51	(0.76)	25	62	0.97	(0.84)	11	109
Average over HN with $\tau > 100$ ps		1.38		12.6	252	1.33		13.1	237
Average over O with $\tau > 100$ ps		1.50		13.2	161	1.69		14.2	219
Average over all HN		0.49		6.5	67	0.56		7.4	64
Average all over O		0.77		8.1	72	0.89		8.9	98

\* $\langle N \rangle$ , average number of urea molecules in the 4 Å sphere.  $^{\dagger}N_v$ , number of different urea molecules visiting the 4 Å sphere.